JMEPEG (2006) 15:287-294
DOI: 10.1361/105994906X108666

1059-9495/$19.00

Forming Limit of Electrodeposited Nickel Coating in the Left Region

L.Q. Zhou, Y.P. Li, and Y.C. Zhou

(Submitted April 29, 2005; in revised form October 31, 2005)

A uniform nickel (Ni) coating was bilaterally electrodeposited on the low-carbon steel substrate for the application of advanced battery shells. Its forming limit was investigated by Hill localized necking theory coupled with finite element simulation and scanning electron microscopy. The effective stress and effective strain in the Ni coating and steel substrate are deduced using Hill's anisotropic yield function. The localized necking condition is derived by sandwich sheet analysis, and the forming limit strains are obtained by solving the nonlinear equation of the localized necking condition. Extensive calculations are carried out using the proposed model. This study exhibits the nickel coating thickness and the normal anisotropic coefficients of the coating and substrate have little influence on the forming limit curve (FLC) in the left region of the coated sheet, but the strain hardening exponents of the coating and substrate have much effect on it. The calculated result matches well with the measured data in uniaxial tension. This investigation is useful for the preparation of the electrodeposited Ni coating and helpful for the forming operation of the battery shells.

Keywords electrodeposited nickel (Ni) coating, forming limit, necking

1. Introduction

Thin coatings have been applied in industry for a wide range of engineering purposes. The evaluation and enhancement of the mechanical reliability of these inhomogeneous structures have emerged as high priorities in both materials science and solid mechanics communities. Coated and precoated metals are resistant to pollution, chemicals, corrosion, and heat and have been used in engineering for forming special parts (Ref 1-3). The forming performance of the coating is very attractive because the coating is very thin and would not fracture or flake as the coated sheet deforms. Also, in most cases, the coating film is in contact with dies, and the tensile strength and elongation of the coating are generally lower than that of the substrate. Therefore, the formability of the coated sheet depends more on the coating than on the substrate (Ref 4).

One of the needs of modern sheet metal forming is reliable knowledge about the formability of a given material in a given forming process. The forming limit of sheet metal is defined to be the state at which localized thinning of the sheet initiates during forming, ultimately leading to a split in the sheet. Forming limit curves are very useful for predicting the formability of sheet-metal forming processes and evaluating the workability of sheet metals (Ref 5). The formability of monolithic sheet materials has been studied extensively in recent decades, and current interests have led to several theoretical analyses of sheet metal forming instability based on different models (Ref 6, 7). Strain-based forming limit diagrams (FLD) and stress-based FLD are currently available (Ref 8). The traditional strain-based FLD was first proposed by Keeler and Goodwin and constructed by a large number of combinations of major and minor strains (Ref 9). Hill (Ref 10) originally proposed localized necking along a direction of zero-extension and constructed the left region of the strain-based FLD. Research devoted to study of the left region rather than the right region of the FLD is limited thus far (Ref 11-13).

A steel sheet with an electrodeposited nickel (Ni) coating was prepared, and the materials were used in advanced structure applications after special heat treatment. The materials were dynamically impacted by projectiles from a 57 mm light air cannon, and it was found that the Ni electrodeposited steel sheet had better interface quality than predeposited SPCC made abroad (Japan) (Ref 14). The stress-strain relations of the electrodeposited Ni coating and the steel substrate were determined using a JEOL JSM-5600LV (Tokyo, Japan) scanning electron microscope (SEM) in which the applied tensile force could be produced by tensile equipment. To study the formability of the materials for deep drawing of advanced battery shells, in this paper, the forming limits of the coated sheet in the negative minor-strain region were investigated with Hill's plastic instability theory, using sandwich sheet analysis.

A bilaterally coated sheet may be considered as a kind of composite material, just like a sandwich sheet. Semiatin et al. (Ref 15) studied the forming limit of sandwich sheet with punch-forming experiments on stainless steel clad aluminum. Recently, Yoshida et al. and Peng et al. (Ref 16, 17) using an approach based on Hill's anisotropic plasticity, studied the forming limits of stainless-steel/aluminum sheet laminates. In this research, this method is adopted for analyzing a sandwich sheet for construction of the forming limits of the bilateral coated sheet and for analysis of the formability of the electrodeposited Ni coating.

L.Q. Zhou and **Y.P. Li,** Mechanical Engineering School of Xiangtan University, Hunan, 411105, China; **Y.C. Zhou,** Key Laboratory of Advanced Materials and Rheological Properties of Ministry of Education, Xiangtan University, 411105, Hunan, China. Contact e-mail: johnzlq@163.com.

2. Effective Stress and Effective Strain of the Coated Sheet

The original form of the Hill's yield function was given as (Ref 18):

$$2f(\sigma_{ij}) = F(\sigma_y - \sigma_z)^2 + G(\sigma_z - \sigma_x)^2 + H(\sigma_x - \sigma_y)^2 + 2L\tau_{yz}^2 + 2M\tau_{zx}^2 + 2N\tau_{xy}^2 = 1 \quad \text{(Eq 1)}$$

where F, G, H, L, M, and N are anisotropic constants of the materials. These constants can be determined by mechanical testing.

By selecting the coordinate axes x, y, and z as the principal stress axes 1, 2, and 3, the effective stress becomes (Ref 19):

$$\overline{\sigma} = \frac{\sqrt{3}}{2}\left[\frac{F(\sigma_2 - \sigma_3)^2 + G(\sigma_3 - \sigma_1)^2 + H(\sigma_1 - \sigma_2)^2}{F + G + H}\right]^{1/2} \quad \text{(Eq 2)}$$

where σ_1, σ_2, and σ_3 are principal stresses in axes 1, 2, and 3, respectively.

Similar to the plastic theory of isotropic materials, when neglecting the elastic strain increment, the relation of the plastic strain increment $d\varepsilon_{ij}$ with the stress σ_{ij} is:

$$d\varepsilon_{ij} = d\lambda \frac{\partial f(\sigma_{ij})}{\partial \sigma_{ij}} \quad \text{(Eq 3)}$$

Thus, the effective strain increment is:

$$d\bar{\varepsilon} = \left[\frac{2}{3}\frac{F + G + H}{FG + GH + HF}(F(d\varepsilon_1)^2 + G(d\varepsilon_2)^2 + H(d\varepsilon_3)^2)\right]^{1/2} \quad \text{(Eq 4)}$$

where ε_1, ε_2, and ε_3 are principal strains in axes 1, 2, and 3, respectively.

In sheet-forming operations, the stress in the thickness direction is usually less than 5% of the in-plane stresses and is usually disregarded (Ref 15). Letting the thickness direction be the third axis, it is assumed $\sigma_3 = 0$, and Eq 2 becomes:

$$\overline{\sigma} = \frac{\sqrt{3}}{2}\left[\frac{\frac{F}{G}\sigma_2{}^2 + \sigma_1{}^2 + \frac{H}{G}(\sigma_1 - \sigma_2)^2}{\frac{F}{G} + 1 + \frac{H}{G}}\right]^{1/2} \quad \text{(Eq 5)}$$

Because the sheet is ordinarily rolled, it is generally in-plane isotropic and normal anisotropic. Thus, $F = G$ and $H/G = H/F = R$; here R is the normal anisotropic coefficient. Let the principal stress ratio be α, that is, $\alpha = \sigma_2/\sigma_1$. Thus, Eq 5 becomes:

$$\overline{\sigma} = \left[\frac{3(1 + R)}{4(2 + R)}\left(1 - \frac{2R}{1 + R}\alpha + \alpha^2\right)\right]^{1/2}\sigma_1 \quad \text{(Eq 6)}$$

Similarly, for the ith layer of the sandwich-coated sheet, the relation of the effective stress, $\overline{\sigma}^{(i)}$ with the principal stress in axis 1 direction, $\sigma_1{}^{(i)}$ is:

$$\overline{\sigma}^{(i)} = B^{(i)}\sigma_1{}^{(i)} \quad \text{(Eq 7)}$$

where

$$B^{(i)} = \left[\frac{3(1 + R^{(i)})}{4(2 + R^{(i)})}\left(1 - \frac{2R^{(i)}}{1 + R^{(i)}}\alpha^{(i)} + \alpha^{(i)^2}\right)\right]^{1/2} \quad \text{(Eq 8)}$$

Equations 7 and 8 explain that, in the sandwich of the coated sheet, the effective stresses in different layers are different.

For the planar isotropic and normal anisotropic monolithic sheet, similarly with R being the normal anisotropic coefficient, the effective strain increment may be obtained by Eq 4, now written as:

$$d\bar{\varepsilon} = \left\{\frac{2}{3}\frac{2 + R}{1 + 2R}[(d\varepsilon_1)^2 + (d\varepsilon_2)^2 + R(d\varepsilon_3)^2]\right\}^{1/2} \quad \text{(Eq 9)}$$

Because the material volume remains constant during plastic deformation, $d\varepsilon_1 + d\varepsilon_2 + d\varepsilon_3 = 0$; that is, $d\varepsilon_3 = -d\varepsilon_1 - d\varepsilon_2$. Letting the strain ratio $\beta = d\varepsilon_2/d\varepsilon_1$ and substituting these relations into Eq 9, the effective strain increment is determined:

$$d\bar{\varepsilon} = d\varepsilon_1\left[\frac{2(2 + R)(1 + R)}{3(1 + 2R)}\left(1 + \frac{2R}{1 + R}\beta + \beta^2\right)\right]^{1/2} \quad \text{(Eq 10)}$$

Hence, for sandwich-coated sheet, in the ith layer, the effective strain increment, $d\bar{\varepsilon}^{(i)}$ with the first principal strain increment $d\varepsilon_1{}^{(i)}$ has the following relation:

$$d\bar{\varepsilon}^{(i)} = C^{(i)}d\varepsilon_1{}^{(i)} \quad \text{(Eq 11)}$$

where

$$C^{(i)} = \left[\frac{2(2 + R^{(i)})(1 + R^{(i)})}{3(1 + 2R^{(i)})}\left(1 + \frac{2R^{(i)}}{1 + R^{(i)}}\beta + \beta^2\right)\right]^{1/2} \quad \text{(Eq 12)}$$

Equations 11 and 12 illustrate that, in the sandwich-coated sheet, the effective strains are different in each layer.

Based on Eq 3, the relationship between the strain increment ratio β and the stress ratio α can be determined as follows:

$$\beta = \frac{\alpha^{(i)}(1 + R^{(i)}) - R^{(i)}}{1 + R^{(i)} - \alpha^{(i)}R^{(i)}} \quad \text{(Eq 13)}$$

When the forming limits in a sandwich-coated sheet forming process are calculated, given the β value, the stress ratio α for the ith layer is:

$$\alpha^{(i)} = \frac{R^{(i)} + (1 + R^{(i)})\beta}{1 + R^{(i)} + \beta R^{(i)}} \quad \text{(Eq 14)}$$

3. Forming Limits of the Coated Sheet

The deformation of materials used in sheet forming applications is most often limited by the onset of instability rather than fracture. The uniaxial true stress-true strain curve is an indispensable tool used to gauge stable as well as unstable flow behavior. The FLD is usually used to characterize the formability of sheet metal. Experimental evidence has shown that

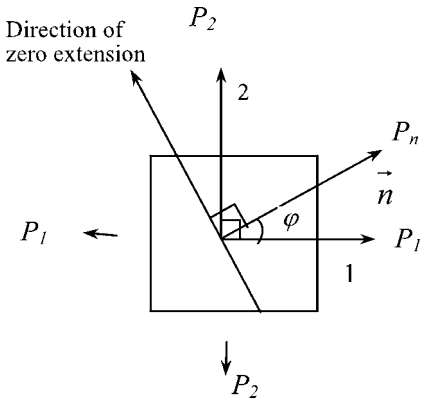

Fig. 1 Localized necking and maximum load

the material properties, sheet thickness, strain paths, and surface finish are the major factors controlling the formability of sheet metals (Ref 18).

3.1 Basic Assumptions

To study the forming limit of the coated sheet, the following general assumptions are made in this research:

- The component is a kind of sheet that is continuous in nature, uniform, and cannot be compressed.
- The interface has enough strength and will not delaminate during plastic deformation. Thus, the strains in the different components are equivalent.
- The influence on the flow stress for the change in the component material at the interface is neglected.

In fact, the results obtained using the above assumptions are demonstrated to agree well with experiments (Ref 15-17, 20).

3.2 Hill Localized Necking Conditions for Coated Sheet

In deep drawing, the instability occurs either as a result of insufficient blank holder force, which gives rise to wrinkling of the flange (Ref 21) or as a result of loss of load carrying ability in the wall, which then leads to localized necking and fracture (Ref 15). For localized necking in a drawing process, the strain ratio β is negative, corresponding to the left region of the FLD.

For a strain ratio in the negative region, the forming limit of a coated sheet may be analyzed using Hill's localized necking criteria. The direction of localized necking is the direction of zero extension (Fig. 1). The condition of the maximum load is perpendicular to the direction of zero extension,

$$dP_n = \sum_i (\sigma_n^{(i)} A_n^{(i)}) = 0 \qquad \text{(Eq 15)}$$

where $A_n^{(i)}$ is the cross-section area of ith layer of the coated sheet in the direction $\vec{n}$. $\vec{n}$ is the direction perpendicular to the direction of zero extension.

$$\because \frac{dA_n^{(i)}}{A_n^{(i)}} = -d\varepsilon_n$$

Thus, Eq 15 becomes:

$$dP_n = \sum_i A_n \xi^{(i)} (d\sigma_n^{(i)} - \sigma_n^{(i)}\, d\varepsilon_n) = 0 \qquad \text{(Eq 16)}$$

In Eq 16, A_n is the cross-section area of the coated sheet in direction $\vec{n}$, and $\xi^{(i)}$ is the ratio of ith layer thickness in total thickness of the coated sheet. Because the volume of the component remains constant during deformation according to our assumption, and the strains in each layer are equal, $\xi^{(i)}$ does not change when the coated sheet deforms. Therefore,

$$\sum_i \xi^{(i)} \left(\frac{d\sigma_n^{(i)}}{d\varepsilon_n} - \sigma_n^{(i)} \right) = 0 \qquad \text{(Eq 17)}$$

The angle φ to the $\vec{n}$ direction may be determined when the strain increment is equal to zero in the direction of zero extension. Thus:

$$tg^2\varphi = -\frac{d\varepsilon_2}{d\varepsilon_1} = -\beta \qquad \text{(Eq 18)}$$

and

$$\varphi = \pm arctg \sqrt{-\beta} \qquad \text{(Eq 19)}$$

The stress $\sigma_n^{(i)}$ lies in the direction perpendicular to the localized necking and may be derived using the relation of $\sigma_n^{(i)}$ with $\sigma_1^{(i)}$ and σ_2. Thus, we obtain:

$$\sigma_n^{(i)} = \frac{(1+\beta)(1+R^{(i)})}{1+R^{(i)}+\beta R^{(i)}} \sigma_1^{(i)} \qquad \text{(Eq 20)}$$

letting:

$$D^{(i)} = \frac{(1+\beta)(1+R^{(i)})}{1+R^{(i)}+\beta R^{(i)}} \qquad \text{(Eq 21)}$$

and substituting Eq 7 and 21 into Eq 20, we obtain:

$$\sigma_n^{(i)} = D^{(i)}/B^{(i)} \cdot \bar{\sigma}^{(i)} \qquad \text{(Eq 22)}$$

In addition, the strain increment in the direction perpendicular to the localized necking may be derived using the relationship between $d\varepsilon_1$, $d\varepsilon_2$, and $d\varepsilon_3$. That is:

$$d\varepsilon_n = (1+\beta) d\varepsilon_1$$

$$\because d\varepsilon_1 = d\varepsilon_1^{(i)} \qquad \text{(Eq 23)}$$

Using this equation and Eq 11, and substituting into Eq 23:

$$d\varepsilon_n = \frac{1+\beta}{C^{(i)}} d\bar{\varepsilon}^{(i)} \qquad \text{(Eq 24)}$$

By substituting Eq 22 and 24 into Eq 17, the following is obtained:

$$\sum_i \xi^{(i)} \frac{D^{(i)}}{B^{(i)}} \left[\frac{C^{(i)}}{1+\beta} \frac{d\bar{\sigma}^{(i)}}{d\bar{\varepsilon}^{(i)}} - \bar{\sigma}^{(i)} \right] = 0 \qquad \text{(Eq 25)}$$

The strain hardening power law was adopted for each layer of the coated sheet. For the *i*th layer, it is:

$$\overline{\sigma}^{(i)} = K^{(i)}\bar{\varepsilon}^{(i)n(i)} \quad \text{(Eq 26)}$$

where $n^{(i)}$ is the strain-hardening exponent of material *i*, and $K^{(i)}$ is the strength constant of the material.

Substituting Eq 26 into Eq 25, it can be seen that:

$$\sum_i \xi^{(i)} \frac{D^{(i)}}{B^{(i)}} K^{(i)}\bar{\varepsilon}^{(i)n(i)} \left[\frac{C^{(i)}n^{(i)}}{(1+\beta)\bar{\varepsilon}^{(i)}} - 1 \right] = 0 \quad \text{(Eq 27)}$$

Equation 27 is the localized necking condition for a coated sheet. By giving the materials parameters and strain path β, the coefficients $\xi^{(i)}$, $B^{(i)}$, $C^{(i)}$, and $D^{(i)}$ may be determined. Thus, Eq 27 is a nonlinear equation of unknown parameter $\bar{\varepsilon}^{(i)}$. For the coated sheet, Eq 27 contains the coating's effective strain $\bar{\varepsilon}_c$ and the substrate's effective strain $\bar{\varepsilon}_s$. Combined with assumption *b*, namely that the principal strains in the coating and substrate are equal, the nonlinear equation (i.e., Eq 27) may be solved.

4. Results and Discussion

An electrodeposited Ni coating on low-carbon steel sheet was prepared in the authors' laboratory. The steel substrate thickness was 0.25 mm. The Ni coating was bilaterally deposited on the substrate, and the thickness of the Ni coating is 3-10 μm. The stress-strain relation of electrodeposited Ni coating was tested in the SEM, in which the applied tensile force could be applied to the sample using a tensile straining device. With the method, the stress-strain properties of substrate without coating were first determined. After that, the stress-strain properties of the coating with substrate were determined. Then the stress-strain relation of the coating was calculated using a mechanical model (Ref 22). The test data were fit by exponential curves using the least squares method. That is, $\sigma = 946.3\varepsilon^{0.3696}$ (MPa) for the low-carbon steel substrate, and $\sigma = 1805.6\varepsilon^{0.3570}$ (MPa) for the Ni coating. In the experiment, the surface of the specimen was examined using SEM while the specimen was loaded. In this case, the initiation of microcracks and the propagation of macrocracks could be observed.

To investigate the forming limits for the coated sheet in the left region of the forming limit diagram, Eq 27 was solved first. Equation 11 was then used to transfer the coating's effective strain $\bar{\varepsilon}_c$ and the substrate's effective strain $\bar{\varepsilon}_s$ in Eq 27 into the principal strain ε_1. Thus, Eq 27 becomes a nonlinear equation related to one unknown parameter ε_1, and it may be solved by the half-interval method. The unknown root for the principal strain ε_1 may be set to the interval [0.001, 3.0], and the convergence precision may be specified as 10^{-4}. For the strain path, $-0.9 < \beta < 0$, the solution is very good. According to the proposed model, extensive calculations are carried out on Matlab as follows.

Figure 2 is the calculated forming limit curve of the coated sheet compared with the forming limit curves of the monolithic Ni coating and monolithic steel substrate. The thicknesses of the Ni coating and steel substrate are 10 μm and 0.25 mm, respectively. The calculations of the forming limits for the monolithic coating and substrate are based on typical formulae (Ref 13). That is, the limit strains are:

$$\varepsilon_1^* = n/(1+\beta)$$

$$\varepsilon_2^* = \beta\varepsilon_1^*$$

for normal anisotropic layers. Here *n* stands for the strain hardening exponent of the material. The normal anisotropic coefficient for steel substrate is 1.41 (Ref 23).

Because the strain hardening exponent, or elongation, for the Ni coating is lower than that of low-carbon steel substrate, the forming limit (curve) of the Ni coating is lower than that of the substrate. The forming limit (curve) of the coated sheet lies between them, which can be seen clearly by enlarging the drawing. But it is very close to the forming limit curve of the substrate because the substrate is much thicker than the Ni coating, and the deformation and strength of the coated sheet mainly depend on the substrate.

The effective strains in the Ni coating and steel substrate are generally different and the size is concerned with the strain path (Fig. 3). The strain path is varied when the substrate and

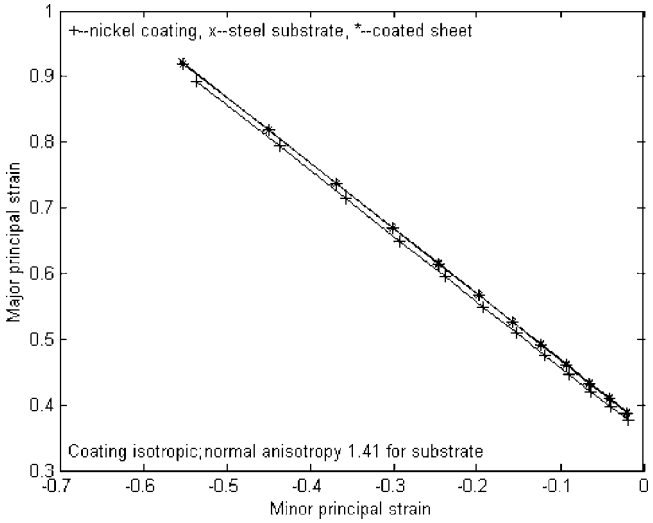

Fig. 2 Forming limit curves of the coating, substrate, and the coated sheet

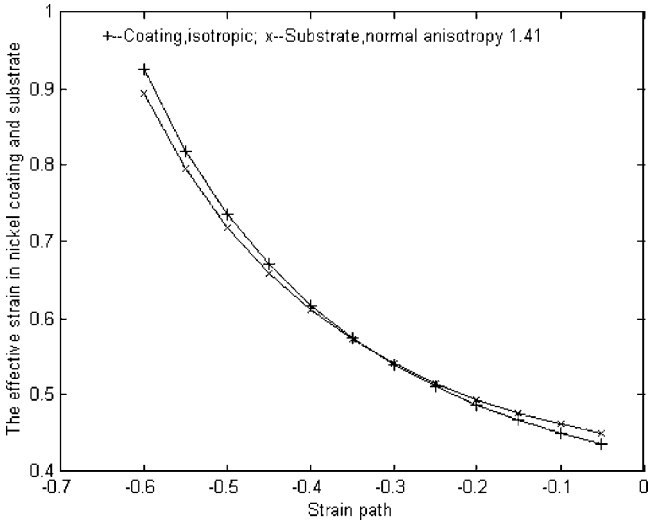

Fig. 3 Effective strains under different strain paths

Fig. 4 Effective strain in steel substrate with a punch stroke of 12.5 mm

Fig. 5 Effective strain in Ni coating with a punch stroke of 10 mm

Table 1 Test procedure parameters

Diameter of punch	Punch fillet radius	Die fillet radius	Blank diameter	Punch stroke	Substrate thickness	Coating thickness
∅ 31 mm	5 mm	5 mm	∅ 55 mm	20 mm	0.25 mm	3 μm

coating are drawn into the battery shell, which may be seen from finite-element method simulated results. The procedure parameters of the punch, die, and the coated sheet used in the simulation are given in Table 1. Figures 4 and 5 are the simulated effective strains in the steel substrate and Ni coating. From the simulation results, the maximum effective strains in the coating and substrate continuously increase with the advance of the punch, i.e., with the time history. Maximum effective strains always lie in the die fillet. The maximum effective strains in the steel substrate with the variation of the punch stroke are shown in Table 2. The maximum effective strain in the Ni coating corresponds with that in the steel substrate.

The proposed model may be examined by performing a uniaxial tensile experiment in the SEM. As mentioned previously, the initiation of microcracks and the propagation of macrocracks could be observed in the SEM. Thus, the initiation of the local necking under uniaxial tension may be easily seen.

Figure 6 is a typical photomicrograph of microcrack initiation on the surface of electrodeposited Ni coating. The steel substrate is not yet fractured. When the tensile load is further increased, the microcrack develops into a macrocrack, resulting in the fracture of the coated sheet. The microcrack direction with respect to the loading direction is measured at 51°, which is consistent with the Hill zero extension. In uniaxial tension, $\beta = -0.5$ for the strain rate. By using Eq 19, the direction of zero extension with respect to the loading direction is ±54° 44′. Thus, the microcrack is produced as a result of local necking. In the experiment, the thicknesses of the Ni coating and steel substrate are 3 μm and 0.25 mm, respectively. Consider the normal anisotropy of 1.41 for the substrate, the limit strain in tensile direction i.e., ε_1 is 0.736 using the proposed model. A value of 0.719 was found through SEM and matches well with the calculated result. Thus, the proposed model provides reasonable agreement.

Figures 7 and 8 show the effect of the substrate and coating

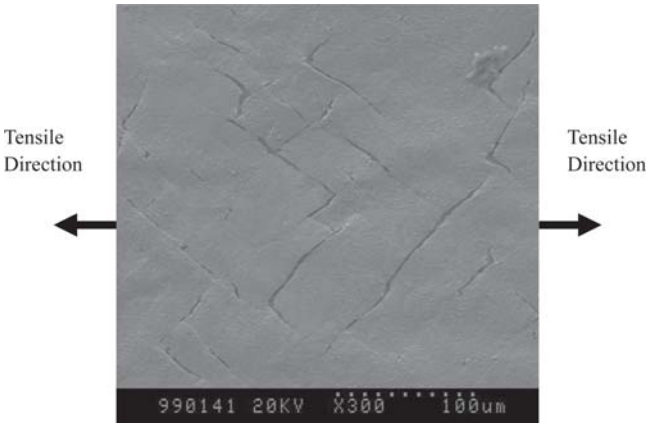

Fig. 6 Micrograph of microcracks initiation in electrodeposited Ni coating loaded by applied force

Table 2 Maximum effective strain in the steel substrate

Time history, ms	4.8	6	7.4	8.6
Punch stroke, mm	7.5	10	12.5	15
Maximum effective strain	0.139	0.229	0.311	0.727

anisotropy on the FLD of the left region. From the graphs in these figures, the normal anisotropy of the layers does not appear to influence the FLD of the left region. This is consistent with the previous results (Ref 24). The normal anisotropy of the substrate has influence on the substrate's effective strain (Fig. 9), but has little influence on the coating's effective strain (Fig. 10). This may be because the Ni coating is only 3 μm thick.

The way in which the Ni coating thickness affects the FLD is shown in Fig. 11. From the calculated data, Ni coating thickness has little effect on its FLD. Strictly speaking, by enlarging the drawing it was found that the thinner the coating is, the better the FLD is for the coated sheet. This arises because the FLD of the Ni coating is lower than that of the steel substrate, and the thinner the coating is, the closer the FLD of the coated sheet is to that of the substrate. But the Ni coating cannot be too thin because it will thin more during the drawing processes (Ref 22).

What largely affects the forming limit is the strain harden-

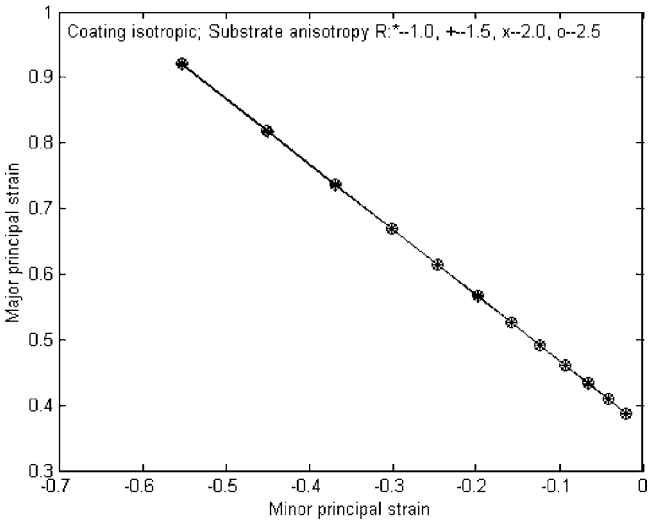

Fig. 7 Effect of the substrate anisotropy on the FLD of the left region

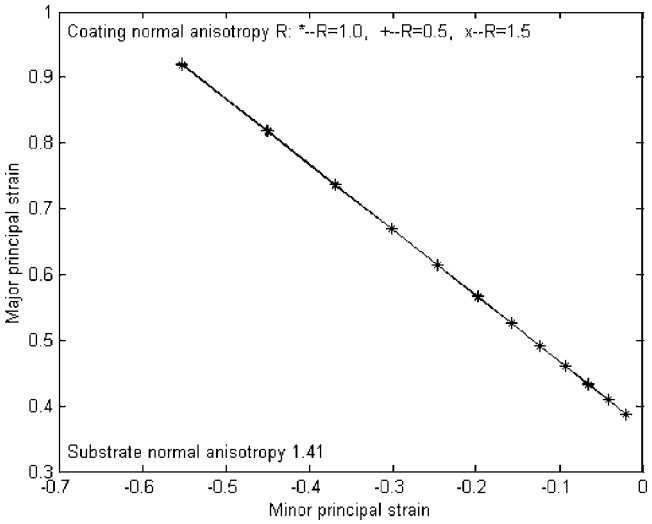

Fig. 8 Effect of the coating anisotropy on the FLD of the left region

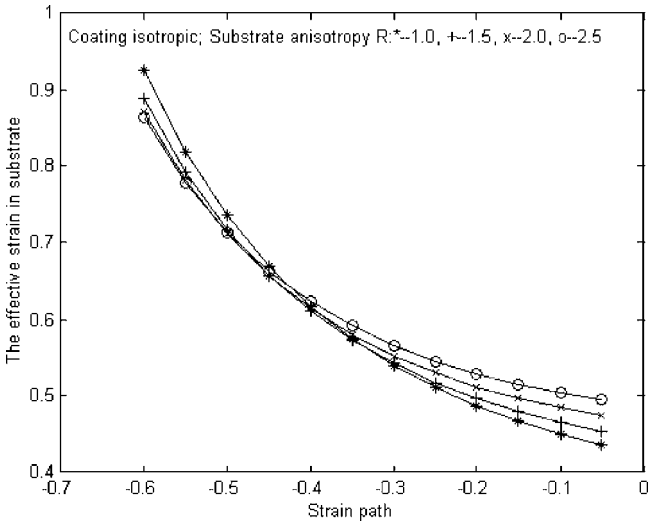

Fig. 9 Effect of the substrate anisotropy on the effective strain in substrate

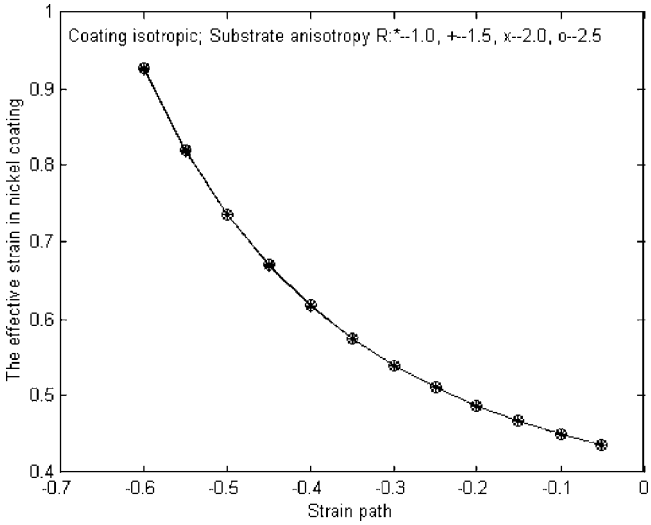

Fig. 10 Effect of the substrate anisotropy on the effective strain of Ni coating

ing exponent, as shown by Fig. 12 and 13. The bigger the strain hardening exponent of the coating or substrate, the higher is the forming limit of the coated sheet. The reason this occurs is that in the same strain path, the higher the strain hardening exponent, the greater the effective strain becomes, which can be seen in Fig. 14 and 15. Thus, the larger the major strain ε_1 is from Eq 11, the higher the forming limit is. From a comparison of Fig. 7, 8, and 11-13, it can be seen that an effective way to improve the forming limit of the coated sheet is to improve the strain hardening exponent of the Ni coating or the steel substrate.

5. Conclusions

A uniform electrodeposited Ni coating was prepared on the substrate of low-carbon steel, suitable for deep drawing into advanced battery shells. The formability of the coated sheet was studied using the forming limit diagram coupled with finite-element analysis and SEM experimentation and examination. The main results obtained in the present investigation can be summarized as follows:

- The forming limit of the Ni coating is lower than that of the steel substrate. The FLC of the coated sheet is between that of the FLC of the coating and the substrate, and is very close to the FLC of the substrate.
- The normal anisotropic coefficient of the Ni coating and steel substrate has no apparent effect on the FLC of the coated sheet. The Ni coating thickness also has little effect on it.
- The strain hardening exponent of the Ni coating and steel substrate has a large effect on the FLC of the coated sheet. The larger the strain hardening exponent of the coating or the substrate, the better the forming limit is for the coated sheet.
- SEM in-situ tensile straining tests show that the proposed model is valid.

Acknowledgments

This work was supported by Hunan Provincial Natural Science Foundation of China (No. 04JJ40035), and the 863 Project

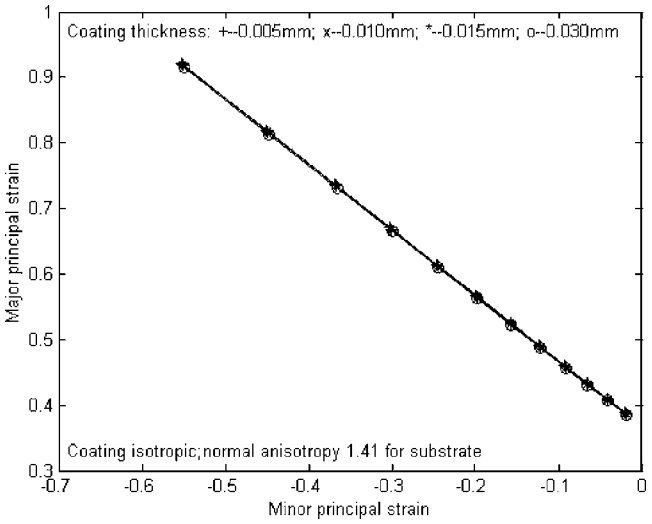

Fig. 11 Effect of coating thickness on the FLD of the left region

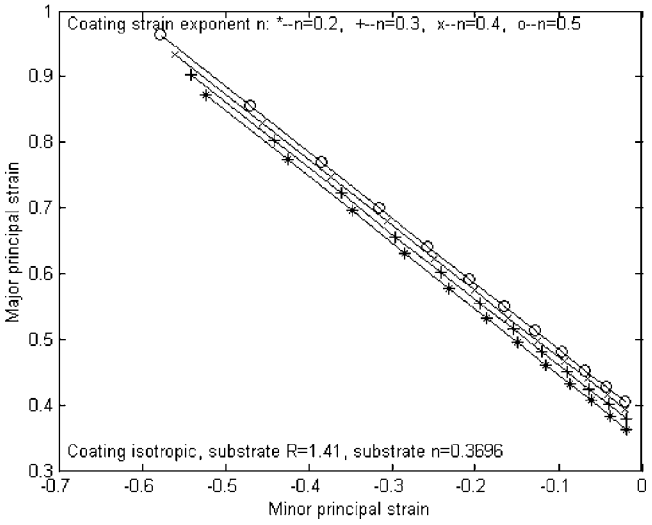

Fig. 12 Effect of the coating strain hardening exponent on the FLD of the left region

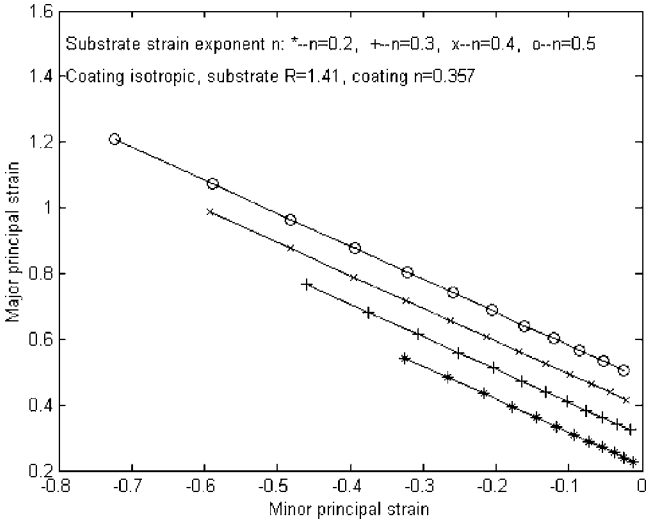

Fig. 13 Effect of the substrate strain hardening exponent on the FLD of the left region

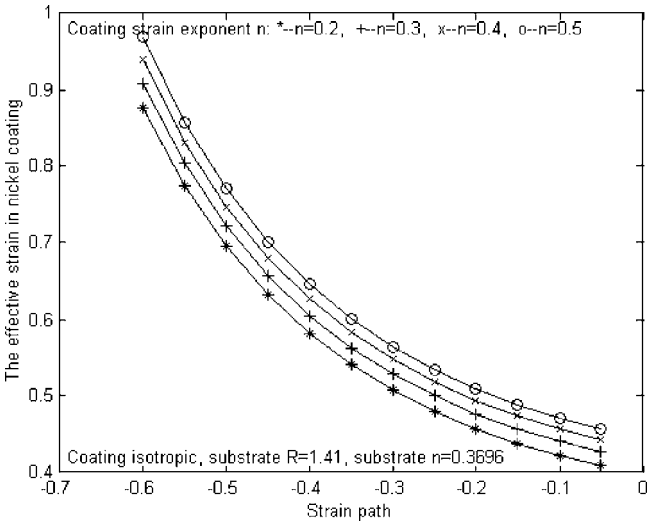

Fig. 14 Effect of the coating's strain hardening exponent on the effective strain

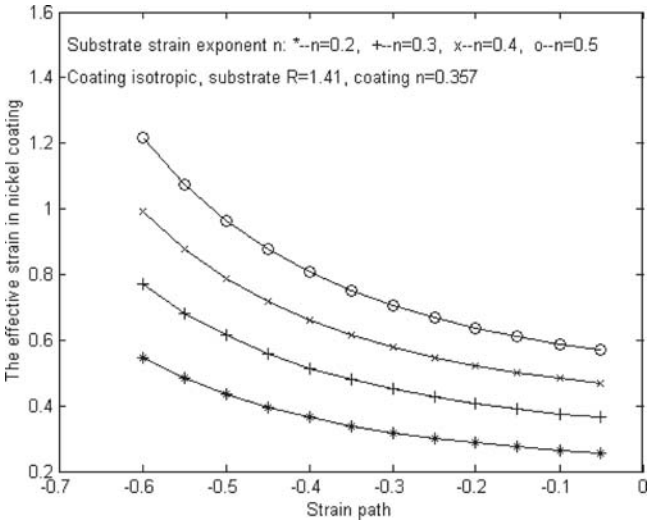

Fig. 15 Effect of the substrate's strain hardening exponent on the effective strain

of China (No. 2003AA331090). The supports are gratefully acknowledged.

References

1. A.G. Mamalis, D.E. Manolakos, and A.K. Baldoukas, On the Finite-Element Modeling of the Deep-Drawing of Square Sections of Coated Steels, *J. Mater. Process. Technol.,* 1996, **58,** p 153-159
2. A.G. Mamalis, D.E. Manolakos, and A.K. Baldoukas, Finite-Element Modeling of the Stretch Forming of Coated Steels, *J. Mater. Process. Technol.,* 1997, **68,** p 71-75
3. K.D. Wit, A.D. Boeck, and B.C.D. Cooman, Study of the Influence of Phase Composition and Iron Content on the Formability Characteristics of Zinc-Iron Electroplated Sheet Steel, *J. Mater. Eng. Perform.,* 1999, **8**(5), p 531-537
4. H.Y. Kim, B.C. Hwang, and W.B. Bae, An Experimental Study on Forming Characteristics of Pre-coated Sheet Metals, *J. Mater. Process. Technol.,* 2002, **120,** p 290-295
5. L.M. Smith, R.C. Averill, J.P. Lucas, T.B. Stoughton, and P.H. Matin, Influence of Transverse Normal Stress on Sheet Metal Formability, *Int. J. Plast.,* 2003, **19**(10), p 1567-1583
6. Hashiguchi, K. and Protasov, A., Localized Necking Analysis by the

Subloading Surface Model with Tangential-Strain Rate and Anisotropy, *Int. J. Plast.,* 2004, **20**(10), p 1909-1930
7. X. Zhu, K. Weinmann, and A. Chandra, A Unified Bifurcation Analysis of Sheet Metal Forming Limits, *J. Eng. Mater. Technol., ASME,* 2001, **123**(3), p 329-333
8. Stoughton, T.B. and Zhu, X., Review of Theoretical Models of the Strain-Based FLD and Their Relevance to the Stress-Based FLD, *Int. J. Plast.,* 2004, **20**(8-9), p 1463-1486
9. Z. Wang, Forming Limits for Sheet Metals Under Tensile Stresses, *J. Mater. Process. Technol.,* 1997, **71,** p 418-421
10. R. Hill, On Discontinuous Plastic States, with Special Reference to Localized Necking in Thin Sheets, *J. Mech. Phys. Solids,* 1952, **1,** p 19-30
11. G.N. Chen, H. Shen, and S.G. Hu, Instability Behavior of Metal Sheets and Limit Strains on the Left of FLD, *Chin. J. Mech. Eng.,* 1993, **29**(3), p 52-58
12. J. Lian and B. Baudelet, Forming Limit Diagram of Sheet Metal in the Negative Minor Strain Region, *Mater. Sci. Eng.,* 1987, **86,** p 137-144
13. K.S. Chan, D.A. Koss, and A.K. Ghosh, Localized Necking of Sheet at Negative Minor Strains, *Metall. Trans. A,* 1984, **15A,** p 323-329
14. L.Q. Zhou, Y.C. Zhou, and Y. Pan, Impact Performance of Electrodeposited Nickel Coating on Steel Substrate, *J. Mater. Sci.,* 2004, **39,** p 753-755
15. S.L. Semiatin and H.P. Piehler, Forming Limits of Sandwich Sheet Materials, *Metall. Trans. A,* 1979, **10A,** p 1107-1118
16. F. Yoshida and R. Hino, Forming Limit of Stainless Steel-Clad Aluminum Sheet under Plane Stress Condition, *J. Mater. Process. Technol.,* 1997, **63,** p 66-71
17. Z.H. Peng and X.F. She, Theoretical Analysis and Experiment on Pressing Forming Limit Strain of Stainless-Steel Clad Aluminum, *Chin. J. Nonferrous Metals,* 1999, **9**(2), p 305-312
18. S. Xu and K.J. Weinmann, On Predicting Forming Limits Using Hill's Yield Criteria, *J. Mater. Eng. Perform.,* 2000, **9**(2), p 174-182
19. Z. Wang, T.D. Guan, J.R. Xiao, P. Lei, and W.C. Huo, Metal Plastic Forming Theory, *Chin. Machine. Press,* 1989, **463-467,** p 476-479
20. J. Zhao and S.B. Li, Plastic Instability of Laminated Sheet Metal When Stretched, *Chin. J. Mech. Eng.,* 1995, **31**(5), p 102-108
21. J. Cao, Prediction of Plastic Wrinkling Using the Energy Method, *Trans. ASME*, *J. Appl. Mech.,* 1999, **66,** p 646-652
22. L.Q. Zhou, Y.P. Li, and Y.C. Zhou, Numerical Analysis of Electrodeposited Nickel Coating in Multi-step Drawing Processes, *J. Eng. Mater. Technol.,* ASME, 2005, **127**(4), p 233-243
23. H. Takuda, K. Mori, H. Fujimoto, and N. Hatta, Prediction of Forming Limit in Deep Drawing of Fe/Al Laminated Composite Sheets using Ductile Fracture Criterion, *J. Mater. Process. Technol.,* 1996, **60,** p 291-296
24. S.G. Hu, *Sheet Cold Forming Theory,* Beijing: National Defence Industry Press, 1979, p 143-145, in Chinese